Journal of Cellular Physiology

Mitochondrial-Targeted Nitroxides Disrupt Mitochondrial Architecture and Inhibit Expression of Peroxiredoxin 3 and FOXM1 in Malignant Mesothelioma Cells

BRIAN CUNNIFF,[1,2] KIRA BENSON,[1] JASON STUMPFF,[2,3,4] KHENG NEWICK,[1,2] PAUL HELD,[5] DOUGLAS TAATJES,[1] JOY JOSEPH,[6] BALARAMAN KALYANARAMAN,[6] AND NICHOLAS H. HEINTZ[1,2,4]*

[1]*Department of Pathology, University of Vermont College of Medicine, Burlington, Vermont*

[2]*Cell and Molecular Biology Program, University of Vermont, Burlington, Vermont*

[3]*Department of Molecular Physiology and Biophysics, University of Vermont College of Medicine, Burlington, Vermont*

[4]*Vermont Cancer Center, University of Vermont College of Medicine, Burlington, Vermont*

[5]*BioTek Instruments, Winooski, Vermont*

[6]*Department of Biophysics, Free Radical Research Center, Medical College of Wisconsin, Milwaukee, Wisconsin*

Malignant mesothelioma (MM) is an intractable tumor of the peritoneal and pleural cavities primarily linked to exposure to asbestos. Recently, we described an interplay between mitochondrial-derived oxidants and expression of FOXM1, a redox-responsive transcription factor that has emerged as a promising therapeutic target in solid malignancies. Here we have investigated the effects of nitroxides targeted to mitochondria via triphenylphosphonium (TPP) moieties on mitochondrial oxidant production, expression of FOXM1 and peroxiredoxin 3 (PRX3), and cell viability in MM cells in culture. Both Mito-carboxy-proxyl (MCP) and Mito-TEMPOL (MT) caused dose-dependent increases in mitochondrial oxidant production that was accompanied by inhibition of expression of FOXM1 and PRX3 and loss of cell viability. At equivalent concentrations TPP, CP, and TEMPOL had no effect on these endpoints. Live cell ratiometric imaging with a redox-responsive green fluorescent protein targeted to mitochondria (mito-roGFP) showed that MCP and MT, but not CP, TEMPOL, or TPP, rapidly induced mitochondrial fragmentation and swelling, morphological transitions that were associated with diminished ATP levels and increased production of mitochondrial oxidants. Mdivi-1, an inhibitor of mitochondrial fission, did not rescue mitochondria from fragmentation by MCP. Immunofluorescence microscopy experiments indicate a fraction of FOXM1 coexists in the cytoplasm with mitochondrial PRX3. Our results indicate that MCP and MT inhibit FOXM1 expression and MM tumor cell viability via perturbations in redox homeostasis caused by marked disruption of mitochondrial architecture, and suggest that both compounds, either alone or in combination with thiostrepton or other agents, may provide credible therapeutic options for the management of MM.
J. Cell. Physiol. 228: 835–845, 2013.

Mitochondria are dynamic organelles, constantly adapting their structure and function in response to environmental cues and intracellular signals (Mitra et al., 2009; Hamanaka and Chandel, 2010; Antico Arciuch et al., 2012). Beyond their role as the primary source of ATP in the cell, mitochondria have emerged as signaling hubs that regulate normal and pathological cellular processes through redox-responsive signaling cascades, as reviewed in (Hamanaka and Chandel, 2010; Tait and Green, 2010). It has long been appreciated that cancer cells harbor mitochondria with altered energy production and structural aberrations (de Oliveira et al., 2012). The "Warburg effect" first described altered metabolism in malignant tissues that is characterized by increases in aerobic glycolysis, lactic acid production, and loss of oxidative phosphorylation (Diaz-Ruiz et al., 2011). Along with altered energy metabolism, the mitochondria of tumor cells produce increased amounts of oxidants (Fried and Arbiser, 2008; Klaunig et al., 2011), mainly through electron leakage to molecular oxygen in the electron transport chain (ETC) located in the inner mitochondrial membrane. Leakage of electrons from the ETC to molecular oxygen leads to the formation of superoxide radical which is

Additional supporting information may be found in the online version of this article.

Contract grant sponsor: John Sterling Memorial Grant from the Mesothelioma Applied Research Foundation.
Contract grant sponsor: Lake Champlain Cancer Research Organization.
Contract grant sponsor: Vermont Ladies Auxiliary of Veterans of Foreign Wars.
Contract grant sponsor: Vermont Cancer Center.
Contract grant sponsor: NIEHS;
Contract grant number: T32 ES007122-29.

*Correspondence to: Nicholas H. Heintz, Department of Pathology, University of Vermont College of Medicine, 149 Beaumont Avenue, Burlington, VT 05405.
E-mail: nicholas.heintz@uvm.edu

Manuscript Received: 10 September 2012
Manuscript Accepted: 18 September 2012

Accepted manuscript online in Wiley Online Library (wileyonlinelibrary.com): 27 September 2012.
DOI: 10.1002/jcp.24232

spontaneously and enzymatically dismutated to hydrogen peroxide, the primary oxidant capable of freely crossing membranes (Jones, 2006; Rhee, 2006; Janssen-Heininger et al., 2008; Murphy, 2009). Through oxidation of reactive cysteine residues in signaling factors, hydrogen peroxide has been implicated in the modulation of regulatory pathways that control proliferation, apoptosis, metabolism, migration, and survival (Droge, 2002; Jones, 2010). It is important to note that the balance between oxidant production and metabolism, as well as the array of susceptible targets expressed in the cell, is critical in determining phenotypic responses. Moreover, redox-signaling by endogenous hydrogen peroxide involves significant spatial and temporal regulation, as either too little or too much hydrogen peroxide impairs cell cycle progression and viability (Burhans and Heintz, 2009).

Activation of certain oncogenes, such as Ras, leads to increased production of cellular oxidants, a metabolic response that in most normal cells induces senescence (Lee et al., 1999). Tumor cells evade senescence and tolerate constitutive increases in the production of cellular oxidants, either through loss of checkpoint function or adaptive responses, including the up-regulation of anti-oxidant enzymes. Indeed, some tumor types appear to rely on enhanced production of oxidants for viability and other properties of malignancy (Fried and Arbiser, 2008; Gupta et al., 2012). FOXM1, a redox-responsive transcription factor that regulates genes involved in S phase and the G2/M transition, functions at the interface between oxidative stress, aging, and cancer (Laoukili et al., 2007; Myatt and Lam, 2007; Park et al., 2009). Because FOXM1 is up-regulated in all carcinomas examined to date, and is expressed only in proliferating cells (Laoukili et al., 2007), FOXM1 has emerged as a promising therapeutic target in cancer treatment (Wang et al., 2010). FOXM1 has also been shown to respond to changes in cellular redox status, with its expression increasing in response to exposure to low levels of exogenous hydrogen peroxide and decreasing following overnight treatment of cells with the free radical scavenger TEMPOL (Park et al., 2009). Through up-regulation of anti-oxidant enzymes that include mitochondrial superoxide dismutase (SOD2) and peroxiredoxin 3 (PRX3), FOXM1 permits cells to escape senescence induced by activated Ras (Park et al., 2009).

Previously, we showed that malignant mesothelioma (MM) cells in culture constitutively produce twofold to threefold more mitochondrial superoxide than non-transformed mesothelial cells, and that compounds that inactivate the major mitochondrial anti-oxidant network of thioredoxin reductase 2 (TR2)—thioredoxin 2 (TRX2)—PRX3 increase mitochondrial oxidative stress and block FOXM1 expression (Newick et al., 2012), albeit through an unknown pathway. Other small molecules that perturb mitochondrial redox status may therefore prove useful for inhibiting FOXM1 expression and the clinical management of MM.

Due to its high negative membrane potential, compounds can be selectively targeted to mitochondria through the conjugation of a triphenylphosphonium (TPP) moiety, which provides a large, dispersed positive charge to the test agent (Murphy, 1997). The selective accumulation of TPP-containing compounds in mitochondria has allowed for targeted delivery of a large number of test agents, with levels that can be 100- to 500-fold higher than the bulk concentration (Murphy, 1997; Dhanasekaran et al., 2005). The higher negative membrane potential of tumor mitochondria also facilitates increased accumulation in tumor cell mitochondria versus normal cell mitochondria (Modica-Napolitano and Aprille, 2001; Millard et al., 2010). In this study we evaluated the activity of two TPP conjugated mitochondrial-targeted nitroxides, Mito-carboxy proxyl (MCP) (Dhanasekaran et al., 2005) and Mito-TEMPOL (MT) (Trnka et al., 2008) on MM tumor cell proliferation and survival (Supplementary Fig. S1). Our results indicate that MCP and MT inhibit FOXM1 expression by inducing marked mitochondrial fragmentation and increased production of mitochondrial oxidants, a phenotypic response that appears distinct from mitochondrial fission. In contrast, the parent compounds, carboxy proxyl (CP), TEMPOL, and TPP alone had no effect on FOXM1 expression, mitochondrial architecture, or cell viability at equivalent concentrations. These observations demonstrate that altered mitochondrial energy and oxidant metabolism in tumor cells is linked to FOXM1 expression, thereby providing a rationale for exploiting this relationship for cancer therapy.

Materials and Methods

Cell lines and cell culture

Two human MM cell lines were used in these studies. HMESO1 (HM) was obtained from J. Testa (Fox Chase Cancer Center, Philadelphia, PA); this cell line was originally isolated by Reale et al. (1987). H2373 was established from human MMs after surgical resection (Pass et al., 1995), and was verified to be mesothelial using a calretinin antibody. Morphologically, in culture HM appears epithelioid, while H2373 has fibrosarcomatoid morphology. LP9, a human mesothelial cell line immortalized with hTERT, was obtained from J. Rheinwald (Dana Farber Cancer Institute, Boston, MA). Cell lines were validated by STR DNA fingerprinting using the Promega CELL ID System (Promega, Madison, WI). The STR profiles are of human origin, and did not match known DNA fingerprints in the Cell Line Integrated Molecular Authentication database (http://bioinformatics.istge.it/clima/), but will serve as a reference for further work. Cells were maintained in DMEM-F12 with hydrocortisone, insulin, transferrin, and selenite with 10% fetal bovine serum (FBS; GIBCO, Grand Island, NY) as previously described (Shukla et al., 2003).

Inhibitors

Mito-Carboxy Proxyl (MCP), Mito-TEMPOL (MT), Carboxy Proxyl (CP), TEMPOL, and Methyl Triphenylphosphonium Chloride (TPP) were synthesized as previously described (Dhanasekaran et al., 2005). Mdivi-1 was purchased from Enzo Life Sciences (Farmingdale, NY). Thiostrepton was purchased from EMD Biochemicals (Billerica, MA). Rotenone was purchased from Sigma (St. Louis, MO). All compounds were re-suspended in molecular grade sterile DMSO.

Immunoblotting

Cell lysates were prepared as previously described (Burch et al., 2004). Protein concentrations were determined using Bradford assays (Bio-Rad, Hercules, CA). For non-reducing gels, dithiothreitol (DTT) was omitted from loading buffer. Lysates (15–20 μg protein/well) were resolved by SDS–PAGE and prepared for immunoblotting as previously described (Phalen et al., 2006). Blots were incubated at 4°C overnight with rabbit anti-FOXM1 K19 polyclonal antibody (Santa Cruz Biotechnology, Santa Cruz, CA) at a 1:500 dilution in blocking buffer, anti-PRX3 monoclonal antibody at a 1:2,000 dilution (Ab Frontier, Seoul, Korea), anti-PRX-SO2/3 antibody at a 1:2,000 dilution (Ab Frontier), or anti-PRX1 polyclonal antibody at a 1:2,000 dilution (Ab Frontier), and after washing protein bands were visualized with the Western Lightning chemiluminescent detection system (Perkin Elmer, Waltham, MA) using secondary antibodies coupled to horse radish peroxidase. Blots were stripped and re-probed with a mouse anti-actin antibody (Millipore, Billerica, MA) to verify equal protein loading. Measurement of PRX3 monomer/dimer ratios by immunoblotting was carried out as described above with sample buffer free of reducing agents.

Detection of oxidant formation

Cells were plated in black-wall, clear-bottom 96-well microplates (Corning, Lowell, MA) and treated the following day for 6 h with indicated compounds in triplicate. Cells were then washed in PBS and loaded with 10 μM Dihydroethidium (Invitrogen) prepared in complete media, and read at $525_{ex}/595_{em}$ using a BioTek Synergy H4 Hybrid microplate reader (BioTek Instruments, Winooski, VT). Plates were then washed and loaded with 4 μg/ml Hoescht 33342 (Invitrogen) for 15 min, washed and read at $350_{ex}/450_{em}$ to normalize for cell number. For staining with nitro blue tetrazolium (NBT; Sigma), cells were plated in 24-well dishes and treated as described in the text. After treatment, cells were washed and incubated with 1.5 mg/ml of NBT in Hanks buffered salt solution (HBSS) at 37°C for 40 min. Cells were subsequently washed with HBSS and fixed in 100% methanol. NBT formazan precipitates were dissolved by adding 280 μl KOH and 240 μl DMSO. The amount of reduced NBT was quantified by reading absorbance at 630 nm. Cells were subsequently stained with DAPI and cell nuclei were counted to control for cell number.

MitoSOX Red flow cytometry

After the indicated treatments cells were loaded with 5 μM MitoSOX Red (Invitrogen) in tissue culture medium for 30 min. Cells were washed with HBSS, collected by brief trypsinization, centrifuged and washed twice in HBSS, and re-suspended in 1% bovine serum albumin (BSA) in HBSS with calcium and magnesium and analyzed by flow cytometry. To monitor oxidized MitoSOX Red, cells were excited at 488 nm and emission was collected in the FL2 channel. Cells without dye and/or treated with menadione were used as controls for each experiment (data not shown). For cell cycle determination Hoescht 33342 (Invitrogen) was included in the incubation with MitoSOX Red and analyzed on a BD LSRII analytical flow cytometer. Hoechst 33342 and MitoSOX Red alone controls were used to confirm specificity of emission (data not shown).

Cell viability assays

Cells were plated in 96-well plates at a density of 1,500 cells per well. The following day, cells were treated with test compounds in complete medium. After 5 days cells were washed with PBS, fixed in 3.7% para-formaldehyde (PFA) and stained for 30 min with 0.1% crystal violet in water. To quantify crystal violet staining, the dye was dissolved in 100% methanol and absorbance was read at 540 nm. Signals were normalized by subtracting the background signal from wells treated in the same fashion, but with no cells.

Measurement of mitochondrial redox status by Mito-roGFP2

Cells were plated in 35-mm glass bottom imaging dishes (MatTek, Ashland, MA) and transiently transfected with pEGFP-R12 (mito-roGFP2) using Lipofectamine 2000 (Invitrogen) according to manufacturer's instructions. pEGFP-R12, which expresses a redox-responsive version of GFP targeted to mitochondria, was a gift from J. A. Melendez (College of Nanoscale Science and Engineering, University at Albany, NY). The following day media was changed to CO_2-independent imaging media (Invitrogen) supplemented with all other components of complete MM media and imaged on a Nikon Ti-E inverted microscope with a 100× 1.49 NA objective in a heated environmental chamber. To determine the oxidation state of the probe, fluorescence images were collected with an Andor iXon X3 EMCCD camera (Andor Technology, Belfast, UK) after excitation with the violet (~400 nm) or teal (~495 nm) outputs from a Spectra X light engine (Lumencor, Beaverton, OR); emission was collected at 525 nm for both excitation wavelengths. Individual cells were imaged every minute for 30 min and the ratio of emission from 400 (oxidized) and 495 (reduced) was measured to determine the relative redox status of the probe in each cell line tested. Quantification of signals was determined using the NIS-Elements software (Nikon Instruments, Melville, NY) and is graphically depicted as the mean of the 400/495 ratio ±SEM.

Measurement of mitochondrial morphology

Cells were plated and transfected pEGFP-R12 (mito-roGFP2) as described above. Cells were imaged every 30 sec for 10 min prior to addition of indicated compound in CO_2 independent imaging media directly to the dish mounted on the microscope. Cells were further imaged for 1-h post-drug addition. Representative images of each cell before and after treatment were used to analyze mitochondrial form factor. Methods for analyzing mitochondria were adapted from Koopman et al. (2005, 2006). Briefly, using ImageJ software (ImageJ, NIH) images were uniformly adjusted for brightness/contrast and a "top-hat" filter was applied to isolate bright mitochondria from background. A threshold was applied to each image equally and individual particles (mitochondria) were analyzed for area and perimeter. Form factor (F), a measure of mitochondrial length and branching was determined for each image using the equation $F = (\text{perimeter}^2/4\pi \times \text{area})$.

Immunofluorescence microscopy

Cells were plated on 18-mm glass coverslips (Fisher Scientific, Pittsburg, PA) in 12-well dishes and treated with indicated compounds in complete media. Cells were washed once with PBS and fixed in 3.7% paraformaldehyde (PFA) in PBS for 10 min, permeabilized in 0.25% Triton X 100 in PBS for 10 min, and blocked in 1.5% BSA in PBS for 1 h at room temperature (RT). Coverslips were incubated with rabbit anti-FOXM1 c-20 (Santa Cruz Biotechnology, 1:200) and mouse anti-PRX3 (1:200) in 1.5% BSA for 1 h at RT, washed 5 × 5 min with PBS and incubated with secondary goat anti-rabbit 488 (Invitrogen, 1:400) and donkey anti-mouse 594 (Invitrogen, 1:400) antibodies. Coverslips were then washed 5 × 5 min with PBS, with the final wash containing DAPI (Invitrogen, 1:4,000), and mounted on glass slides (Fischer Scientific) with Aqua-Poly/Mount (Polysciences, Inc, Warrington, PA). Images were collected on a Nikon Ti-E inverted microscope with a 60× oil immersion objective as described above. Exposure times were adjusted based on secondary antibody controls.

Transmission electron microscopy

HM cells were grown on Thermanox plastic coverslips (Nalge Nunc International, Rochester, NY), and fixed for 30 min at 4°C in 2.5% glutaraldehyde/1.0% PFA in 0.1 M cacodylate buffer, pH 7.2. After three rinses in 0.1 M cacodylate buffer, the cells were post-fixed in 1% OsO_4 for 1 h at 4°C, rinsed three times in 0.1 M cacodylate buffer, and stored overnight in buffer at 4°C. The following day, the samples were dehydrated in a graded series of ethanol, and infiltrated with and embedded in EMBed-812 resin by placing a BEEM capsule containing resin over areas of the coverslip containing cells. Following polymerization in an oven, the BEEM capsules were pried off of the coverslip by applying gentle pressure. Ultrathin sections (60–80 nm thick) were cut with a diamond knife and retrieved onto nickel 200-mesh copper grids, and contrasted with 2% alcoholic uranyl acetate and lead citrate. The sections were imaged with a JEOL 1400 transmission electron microscope (JEOL USA, Inc., Peabody, MA) operating at 60 kV. Digital images were acquired with an AMT-XR611 11 megapixel ccd camera (Advanced Microscopy Techniques, Danvers, MA), and saved in tiff format (12.2 mB/image).

Results

FOXM1 expression responds to mitochondrial oxidants

Quantification of the reduction of NBT showed HM cells produce more superoxide under standard culture conditions than do LP9 cells (Fig. 1A), in agreement with other studies (Newick et al., 2012). Flow cytometry with the redox-responsive mitochondrial probe MitoSOX Red showed that

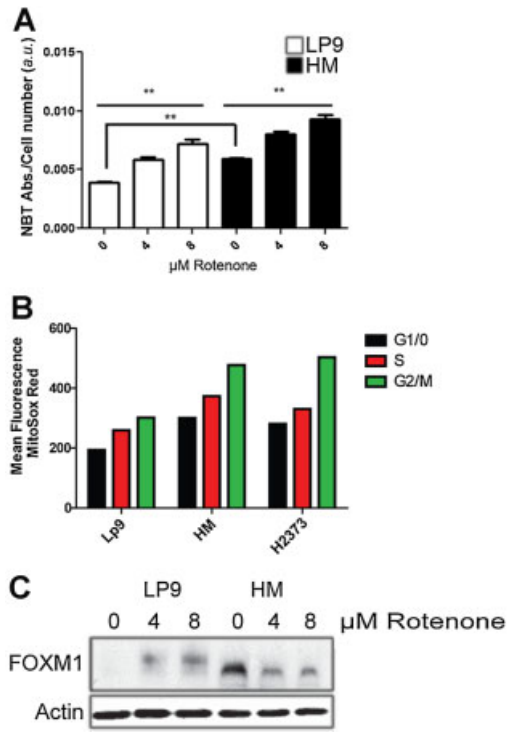

Fig. 1. Rotenone influences FOXM1 expression levels differently in LP9 mesothelial and HM malignant mesothelioma cells. A: Oxidant levels were measured by NBT absorbance as a function of cell number in LP9 and HM cells after treatment for 6 h with the indicated concentration of the complex I inhibitor rotenone. (n = 3, $^{**}P < 0.01$). B: Mitochondrial oxidant levels were measured in the indicated cell lines by flow cytometry with MitoSox Red, using quantification of nuclear DNA content with Hoechst stain to determine cell cycle phase. Shown are the relative levels of mitochondrial oxidants at the G1/0, S, and G2/M phases of the cell cycle. Mitochondrial oxidant levels increase during transition from G0/G1 to G2/M phase in all cell lines, but mitochondrial oxidants are elevated in MM cells as compared to LP9 cells at all phases of the cell cycle. C: Immunoblot analysis shows the effect on FOXM1 expression levels in LP9 and HM cells after treatment with rotenone for 6 h. Actin was used as a loading control. Note the increase of FOXM1 expression in LP9 cells in response to rotenone, whereas the same concentrations of rotenone inhibit FOXM1 expression in HM cells.

production of mitochondrial oxidants was increased at all phases of the cell cycle in two MM cell lines as compared to hTERT-immortalized (but not tumorigenic) LP9 cells (Fig. 1B). Using rotenone, an inhibitor of complex I of the ETC, we examined the relationship between mitochondrial superoxide production and FOXM1 expression in LP9 cells and MM HM cells. Cells were treated with increasing concentrations of rotenone, and superoxide production was measured by the reduction of NBT. In both cell lines, rotenone increased the rate of NBT reduction, most likely by blocking electron flow from complex I (Friedrich et al., 1994; Koopman et al., 2005). However, in LP9 cells, which siRNA experiments showed express a larger isoform of FOXM1 than HM cells (Newick et al., 2012), expression of FOXM1 increased in response to rotenone, whereas in HM cells expression of FOXM1 decreased (Fig. 1C). These results suggest that expression of FOXM1 is tuned to the production of cellular oxidants that include mitochondrial superoxide and hydrogen peroxide or oxidants formed there from, but that tumor cells function closer to a threshold of oxidant production that inhibits FOXM1 expression.

MCP and MT induce a dose-dependent increase in mitochondrial oxidant levels in MM cells

Although MCP and MT have been described to act as antioxidants in a number of in vitro and cellular systems (Dhanasekaran et al., 2005; Weinberg et al., 2010; Khan et al., 2011), changes in mechanism of action as a function of dose are still poorly understood. There is evidence that TPP compounds with similar properties to MCP and MT can lead to increases in oxidant levels by interacting with complex I at sites similar to those influenced by rotenone, which reduces reverse electron transport while increasing superoxide production from forward electron transport (O'Malley et al., 2006; Mukherjee et al., 2007). To determine if MCP and MT influence oxidant production in MM cells, total cellular superoxide or superoxide-derived oxidant production was examined using DHE fluorescence, which also responds other oxidative events (Kalyanaraman et al., 2011). Cells were incubated with test compounds for 6 h, washed, and loaded with DHE, using co-staining with Hoechst to control for the number of cell nuclei. When normalized to DNA content, MCP and MT led to dose-dependent increases in DHE fluorescence (Fig. 2A); with significant increases occurring at doses as low as 400 nM. These findings have been confirmed by quantifying the reduction of NBT in response to test compounds, and flow cytometry with Peroxycrimson (Miller et al., 2007), a fluorescent probe that directly reacts with hydrogen peroxide, albeit slowly, indicating that the majority of mitochondrial superoxide is converted to hydrogen peroxide (data not shown).

To better identify the source of cellular oxidants after MCP or MT treatment, cells were treated with test agents for 6 h as before, loaded with the mitochondrial oxidant probe MitoSOX Red for 30 min, and relative fluorescence was determined by flow cytometry. Both MCP and MT led to dose-dependent increases in MitoSOX Red fluorescence, while CP, TEMPOL and the targeting moiety TPP had no effect on mitochondrial oxidant production at any concentration tested (Fig. 2B). While MitoSOX Red responds to general mitochondrial oxidative stress, together the results with NBT staining and multiple redox-responsive fluorescent probes suggest that nitroxides targeted to MM cell mitochondria with a TPP moiety cause marked increases in mitochondrial superoxide and/or oxidants formed from hydrogen peroxide in MM cells.

To further confirm the increase in oxidative stress after treatment with MCP, protein lysates from treated cells were probed with an antibody that reacts with over-oxidized forms of peroxiredoxins (PRX). Incubation with MCP for 6 h leads to a dose-dependent increase in hyperoxidized PRXs in HM cells (Fig. 2C). PRXs function as obligate homodimers that form disulfide-bonded dimers during the catalytic cycle (Cox et al., 2009a,b). To test if the oxidation state of mitochondrial PRX3 was affected by MCP, non-reducing but denaturing gel electrophoresis conditions were used to examine the ratio of disulphide-bonded PRX3 (e.g., PRX-S-S-PRX3) dimers to PRX3 monomers, which represent either reduced or hyper-oxidized monomers. After 6 h of treatment with MCP, the fraction of mitochondrial PRX3 dimers increased in both HM and H2373 cells (Fig. 2D), indicating increased activity of the PRX3 catalytic cycle, likely due to increased catabolism of hydrogen peroxide. Together the assays for cellular oxidant production provide evidence that MCP and MT lead to increases in mitochondrial oxidative stress in MM cells.

MCP and MT alter mitochondrial architecture

Changes in mitochondrial architecture have been linked to alterations in membrane potential, energy production, and superoxide production (Mitra et al., 2009; Shenouda et al., 2011; Yu et al., 2011; Fischer et al., 2012; Rehman et al., 2012). Using expression of a green fluorescent protein (GFP) targeted

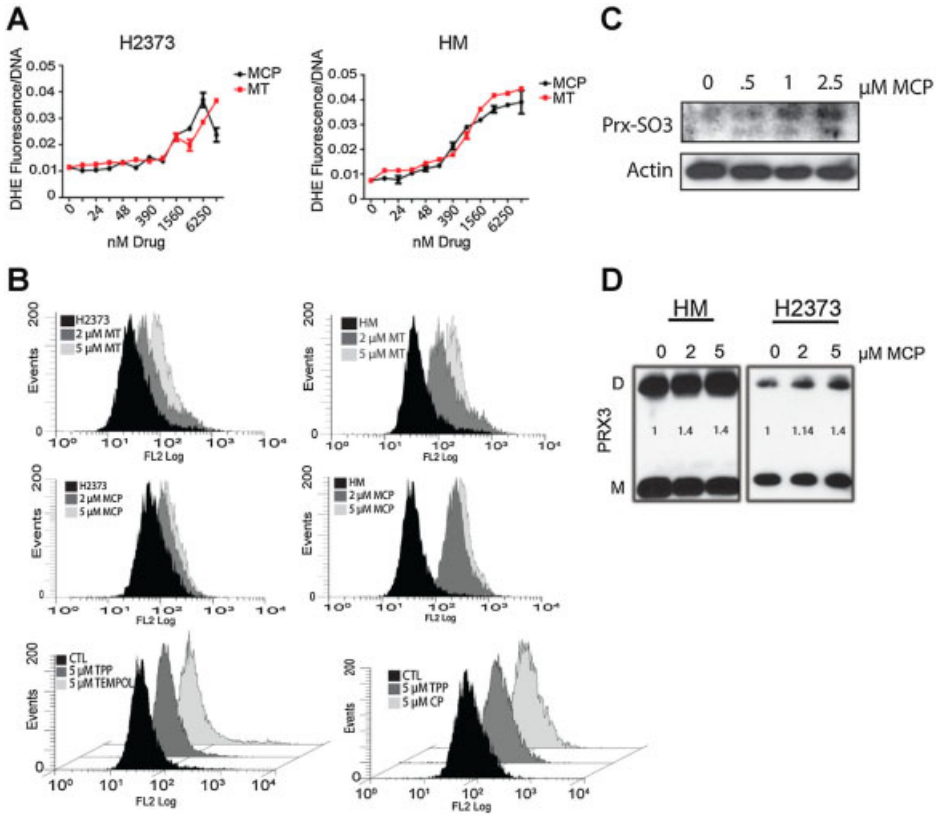

Fig. 2. MCP and MT increase mitochondrial oxidant levels. A: Total cellular oxidant levels were measured by DHE fluorescence after 6 h treatment with MCP or MT in HM and H2373 MM cells. Staining with Hoechst was used to normalize the signals to total cell number. B: Mitochondrial oxidant levels were measured by flow cytometry with MitoSox Red after treatment with MCP, MT or control compounds for 6 h in MM cells. Flow cytometry histograms for TEMPOL, CP, and TTP (bottom two parts) overlaid one another, and are presented in perspective. C: Immunoblot analysis showing hyper-oxidation of peroxiredoxins after treatment with MCP. HM cells were treated with the indicated concentration of MCP for 6 h and total cellular PRX-SO_2H/SO_3 levels were assessed by Western blotting. Actin was used as a loading control. D: Oxidation of mitochondrial localized PRX3 was measured by formation of PRX3-S-S-PRX3 disulfide bonded dimers. HM and H2373 cells were treated with the indicated concentrations of MCP for 6 h, and cell lysates prepared in the absence of DTT but with SDS were resolved by native gel electrophoresis as described in Materials and Methods Section. The relative amount of PRX3-S-S-PRX3 dimers was estimated by Western blotting with an anti-PRX3 antibody. The ratio of dimer to monomer as measured by densitometry is provided.

to the mitochondrial matrix that is responsive to redox status (mito-roGFP2) (Hanson et al., 2004; Cannon and Remington, 2006), and live cell ratiometric imaging to quantify changes in mitochondrial redox status, we investigated the effects of MCP and MT on mitochondrial morphology. HM cells were transfected with the mito-roGFP2 expression vector, and mitochondrial morphology was examined in individual cells for 10 min prior to the addition of test compounds directly to the cell culture on the microscope stage. Images were then collected every 30 sec for 1 h, and videos of individual cellular responses were generated as described in Materials and Methods Section. For each compound, at least 10 individual cells were independently examined in the same dish to judge the uniformity of the response. Within minutes of adding doses as low as 1 μM MCP or MT, mitochondrial architecture was drastically altered in HM cells (Fig. 3A, Supplementary Data Videos 1 and Video 2). Long tubular mitochondria were observed forming circular ring-like structures and vesicles of variable dimensions in a process reminiscent of mitochondrial fission (insets, Fig. 3A). Occasionally long filamentous mitochondria were observed to form lasso-like structures that eventually collapsed into vesicular bodies of varying dimensions. Staining of the nucleus with DAPI showed that in both treated and untreated cells the majority of mitochondria were clustered in the perinuclear region (Fig. 3A and data not shown). An identical morphological response was observed in LP9, H2373, and SKOV3 ovarian cancer cells treated with MCP or MT (data not shown).

To quantify changes in mitochondrial architecture we utilized computer-assisted methods described previously by Koopman et al. (2005). Both MT and MCP led to marked decreases in form factor (Fig. 3B), a measure of mitochondrial length and branching. In contrast, untargeted CP, TEMPOL, and TPP had no effect on mitochondrial architecture (not shown) or form factor (Fig. 3B). To further investigate the mechanism by which MCP alters mitochondrial architecture we used mdivi-1 to inhibit the activity of dynamin-related protein 1 (DRP1), a major regulator of mitochondrial fission (Oettinghaus et al., 2011). By inhibiting fission, mdivi-1 promotes the formation of dense mitochondrial networks (Cassidy-Stone et al., 2008). When HM cells were incubated with mdivi-1 for 3 h and monitored by live cell imaging, mitochondria remained located in the perinuclear region (Fig. 3C) and an increase in form factor was observed (Fig. 3D). After 3 h 1 μM MCP was added directly to plates on the microscope stage and cells were observed for an additional 1 h. Inhibiting mitochondrial fission machinery with mdivi-1 did not attenuate the effect of MCP on mitochondrial architecture (Fig. 3C) or the reduction in form

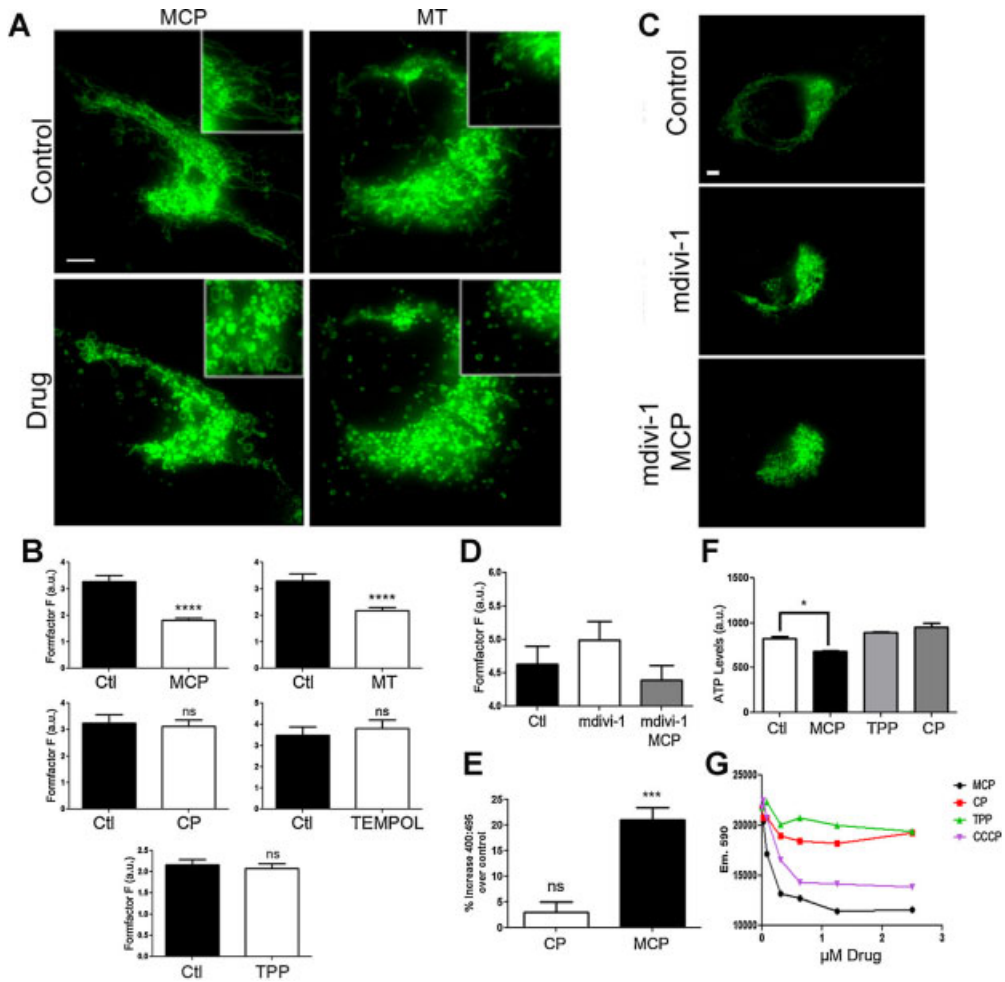

Fig. 3. MCP and MT disrupt mitochondrial architecture. A: HM cells were transfected with mito-roGFP2 and still frame images were captured before (control) and after treatment with 1 μM MCP or MT for 1 h (drug). Enlarged images (insets) represent magnified portions of the same cells (scale bar = 10 μm). Note that MCP and MT induce mitochondrial fragmentation, with vesicular and ring-like structures. Temporal responses in MCP and MT are shown on the supporting imaging videos. B: Quantification of mitochondrial form factor F (as described in Materials and Methods Section) in HM cells treated with MCP or MT, as well as CP, TEMPOL, and TPP controls (n = 10, ****$P = 0.0001$, ns = not significant). C: Still frame images of HM cells transfected with mito-roGFP2 and pre-incubated with the DRP-1 inhibitor mdivi-1 for 3 h (middle part) prior to addition of 1 μM MCP for 1 h (bottom part). Mdivi did not rescue mitochondria from fragmentation by MCP. Scale bar = 10 μm. D: Quantification of mitochondrial form factor from cells presented in C (n = 3). E: Ratiometric imaging of HM cells transfected with mito-roGFP2 was used to quantify increased oxidation in mitochondria as compared to control cells after treatment with 1 μM MCP for 6 h (n = 5, ***$P = 0.0005$). F: Total cellular ATP levels were measured after treatment with 1 μM of the indicated compounds for 6 h (*$P = 0.05$). G: Mitochondrial membrane potential was measured at the indicated concentrations of MCP, CP TPP or the positive control compound CCCP. As compared to CP or TTP, MCP depolarized mitochondrial membranes within 6 h in a dose-dependent fashion, while CP and TPP had no effect on the same end point.

factor (Fig. 3D), suggesting other components of the fission machinery or membrane dynamics disrupted by MCP may be responsible for the architectural aberrations (Manetta et al., 1996). After 6 h with MCP the redox status of mito-roGFP2 was increased over control cells, while CP did not change to redox status of the probe (Fig. 3E), confirming earlier results with other oxidants probes (as in Fig. 2). We also examined if changes in mitochondrial architecture led to changes in ATP levels and disruption of mitochondrial membrane potential, as previously reported (Cheng et al., 2012). Incubation of MM cells with 1 μM MCP led to moderate yet significant decreases in ATP levels after 6 h, with no change in MM cells treated with either TPP or CP at equivalent concentrations (Fig. 3F). MCP, but not CP, also caused marked loss of mitochondrial membrane potential (Fig. 3G).

To gain further insight into structural aberrations caused my MCP we visualized mitochondria of HM cells treated for 6 h with 1 μM MCP or control compounds by transmission electron microscopy. The mitochondrial matrix of MCP-treated cells appeared swollen and devoid of electron density, with loss of mitochondrial cristae, and frequently the inner membrane was closely associated with the outer membrane (Fig. 4). Electron microscopy of MCP-treated cells also showed a preponderance of vesicular mitochondria (Fig. 4, parts D and F), in agreement with the results of live cell imaging. Ultrastructural analysis also suggested that autophagasomes may be increased in MCP-treated cells, an observation that requires further investigation. Control compounds TPP and CP had no visible effect on mitochondria architecture, and other cellular structures (nuclear membrane, plasma membrane, and

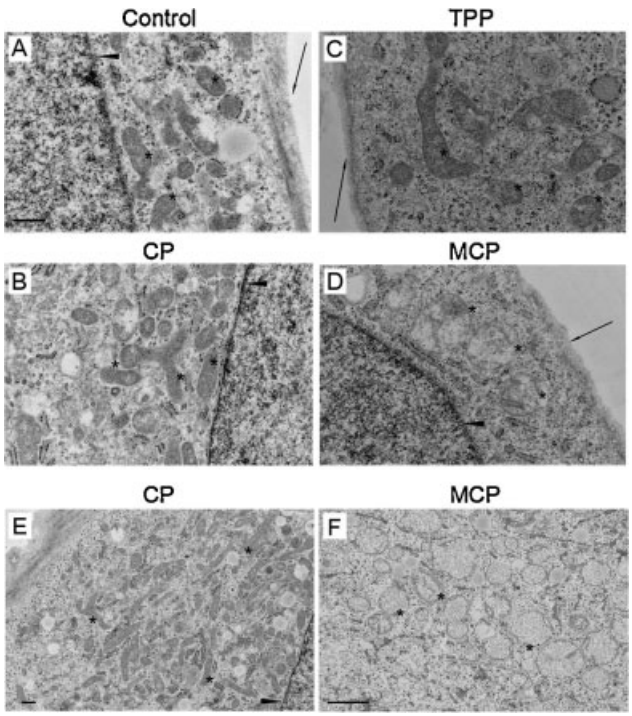

Fig. 4. Mitochondrial architecture by TEM of MCP-treated HM cells. HM cells were incubated for 6 h with 1 μM of indicated compounds and visualized by TEM. Arrows denote the cell membrane, arrowheads denote the nuclear membrane, and asterisks denote mitochondria. Scale bar = 500 nm for (A–E), 2 μm for (F)

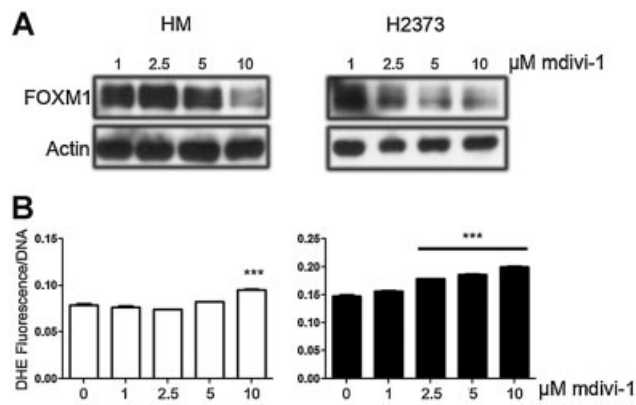

Fig. 5. Mdivi-1 increases mitochondrial oxidant levels and decreases FOXM1 expression in MM cells. A: HM and H2373 cells were incubated with the indicated concentration of the DRP-1 inhibitor mdivi-1 for 12 h and FOXM1 protein expression was evaluated by immunoblotting. B: HM and H2373 cells were treated as in part A and DHE fluorescence was used to measure total cellular oxidant levels. Hoechst staining for DNA content was used to normalize the signal to cell number (n = 3, $P = 0.0001$).

rough ER) appeared largely unaffected by treatment with MCP or control compounds. Together these data indicate that in MM cells MCP and MT promote fragmentation of mitochondria that disrupts multiple aspects of mitochondrial physiology, including ATP production, membrane potential, and oxidant metabolism.

Mdivi-1 inhibits expression of FOXM1

Transitions in mitochondrial morphology, either through increased fission or fusion, can alter the metabolic function of the organelle. It has been reported that mitochondrial oxidants are increased during fission events (Yu et al., 2011), and that fusion can also promote increased oxidant levels and alter ATP production (Mitra et al., 2009; Rehman et al., 2012). Therefore, we investigated the effects of incubation with midivi-1 on oxidant levels and FOXM1 expression in MM cells. Incubation of HM or H2373 cells with mdivi-1 for 12 h led to a dose-dependent loss in FOXM1 protein expression (Fig. 5A), along with a dose-dependent increase in cellular oxidants as measured by DHE fluorescence (Fig. 5B). The loss in FOXM1 protein expression correlated with the increase in oxidant levels in the two MM cell lines tested, further supporting the concept that FOXM1 is responsive to mitochondrial oxidant production. Interestingly, FOXM1 enters the nucleus during G2 in an ERK-dependent manner (Ma et al., 2005), and is degraded during mitosis (Laoukili et al., 2008; Park et al., 2008), two events that are associated with cell cycle-dependent transitions in mitochondrial fission (Berger and Yaffe, 1996; Taguchi et al., 2007) and an increase in the cellular oxidation state (Conour et al., 2004).

MCP causes a loss of PRX3 and FOXM1 protein in MM cells

Given that agents which perturb mitochondrial oxidant production inhibit FOXM1 expression, we examined the effect of manipulating mitochondrial oxidant production with MCP on FOXM1 expression, as well as PRX3, a antioxidant gene product up-regulated by FOXM1 (Park et al., 2009). MM cells were incubated for 12 h with indicated concentrations of MCP or control compounds, and Western blotting was used to assess changes in protein expression. As shown in Figure 6A, both FOXM1 and PRX3 protein expression were reduced in cells treated with MCP, while CP and TPP had no effect at the same concentrations. The loss of mitochondrial PRX3 expression was specific, as expression of cytosolic PRX1 was not affected by MCP (Fig. 6B). Moreover, the loss of FOXM1 and PRX3 expression did not appear to be due to a simple loss of mitochondrial mass, as levels of mitochondrial TR2 were unaffected by MCP (Fig. 6C). Loss of FOXM1 or PRX3 expression was not observed in cells treated with both MCP and MG132 (Fig. 6C), an inhibitor of the proteosome and Lon protease, a mitochondrial protease that prefers oxidized proteins as substrates (Bota and Davies, 2002; Venkatesh et al., 2011). MCP did not affect expression of PRX3 mRNA (not shown).

FOXM1 coexists with mitochondrial PRX3

Given that at least five compounds that perturb mitochondrial redox status or architecture (gentian violet, thiostrepton, MCP, MT, and mdivi-1) decrease the expression of FOXM1 isoforms that migrate at ~105–115 kDa, we investigated the subcellular localization of FOXM1 using immunofluorescence microscopy (IF). Previously we reported that siRNA specific to FOXM1, but not control siRNA, eliminated the expression of immunoreactive species of FOXM1 that migrate at ~105–115 kDa on Western blots (Newick et al., 2012). Using three different FOXM1 antibodies (see Material and Methods Section), and an antibody to PRX3 to define mitochondria, immunofluorescence microscopy of HM cells showed a significant fraction of FOXM1 coexists with PRX3 in HM cells (Fig. 7, column A), suggesting that cytoplasmic FOXM1, which is

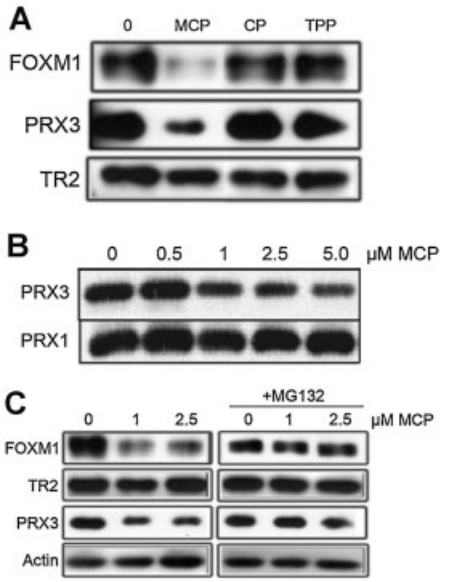

Fig. 6. MCP leads to loss of FOXM1 and PRX3 protein expression in MM cells. A: HM cells were treated with the indicated concentration of MCP, CP, or TPP for 12 h, and FOXM1, PRX3, and TR2 levels were evaluated by immunoblotting. B: HM cells were treated with the indicated concentrations of MCP for 12 h, and PRX3 expression levels were compared to PRX1 by immunoblotting. MCP reduced expression of PRX3 while PRX1 was unaffected. C: HM cells were treated with the indicated concentration of MCP, or MCP plus 10 μM MG132, an inhibitor of the proteosome and Lon protease. FOXM1, PRX3, and TR2 expression levels were evaluated by immunoblotting. Actin was used as a loading control.

observed in human mesothelioma tumor specimens (Newick et al., 2012), may be associated with or located within mitochondria. To test this possibility further, cells were treated with thiostrepton (TS), a thiazole antibiotic which inhibits expression of FOXM1 in a wide variety of cancer cell lines (Bhat et al., 2009; Pandit and Gartel, 2011; Qiao et al., 2012). Immunofluorescence of HM cells treated with thiostrepton showed marked decreases in cytoplasmic staining of FOXM1 without diminishing the signal for PRX3 (Fig. 7, column B), whereas treatment of cells with MCP reduced the immunofluorescence signal for both FOXM1 and PRX3 (Fig. 7, column C), confirming the results observed by immunoblotting (Fig. 6). The subcellular trafficking of FOXM1 from the cytoplasm to the nucleus is regulated during the cell cycle (Ma et al., 2005), and the immunofluorescence results indicate that a significant fraction of cytoplasmic FOXM1 is associated with mitochondria in HM cells. The precursor–product relationship between cytoplasmic FOXM1 observed in tumor specimens or cell lines and nuclear FOXM1 that mediates gene expression, if any, is not known.

MCP inhibits MM cell viability and potentiates the cytotoxic effects of TS

The cationic triphenylmethane gentian violet inhibits expression of TRX2 (Zhang et al., 2011), and TS adducts PRX3 (Newick et al., 2012), indicating that both compounds target mitochondrial antioxidant enzymes that influence the expression of FOXM1 and MM cell viability. To test the effects of MCP on MM cell viability, HM and H2373 cells were treated with low doses of MCP, with or without exposure to either 0.5 or 1 μM thiostrepton, concentrations of TS that are well below the ID_{50} of ~2.3 μM in HM cells (Newick et al., 2012). HM and H2373 cells were plated in 96-well dishes, treated in triplicate for 5 days, washed, and then stained with crystal violet. After washing, the crystal violet was solubilized in 100% methanol and total cell mass was quantified by absorbance at 540 nM (Fig. 8). Additive effects of the two drugs on inhibition of cell growth as reflected by total cell mass were observed in both HM and H2373 cells (Fig. 8A,B). Like gentian violet (Newick et al., 2012), MCP increased the adduction of PRX3 by TS in HM cells (Fig. 8C), suggesting that mitochondrial oxidative stress induced by MCP promote the formation of catalytic intermediates of PRX3 that preferentially react with TS, thereby enhancing the cytotoxic activity of TS. These studies add MT and MCP to the growing list of agents that influence tumor cell viability through perturbations in mitochondrial physiology.

Discussion

Altered metabolism, redox status, and mitochondrial structure have long been hallmarks of malignant transformation, and in the past decade there has been increased interest in exploiting these perturbations for cancer therapy (Ralph et al., 2010). In general, in cancer cells mitochondria do not appear defective in many aspects of energy metabolism, but rather respond to deregulation of the cell cycle and other signaling pathways by exploiting aerobic glycolysis for production of reducing equivalents required for biosynthetic processes and cell cycle progression (de Oliveira et al., 2012). While gaining a better understanding of the alterations in mitochondria and their relationship to malignant phenotypes has been challenging, there remains enthusiasm for testing new avenues to target the altered metabolic and redox status of tumor cells, as these may provide therapeutic targets that are not present in normal cells.

As in other tumor types, we have described an increase in the oxidative state of MM cell mitochondria that is accompanied by an adaptive response of up-regulation of a primary mitochondrial antioxidant network composed of TR2-TRX2-PRX3 (Newick et al., 2012), which is responsible for 90% of the metabolism of mitochondrial H_2O_2 (Cox et al., 2009c). This adaptation permits increased cell proliferation and evasion of apoptosis by shifting redox status in favor of pro-growth oxidant signaling without activating redox dependent pro-apoptotic pathways. Our previous findings have also demonstrated that targeting of the mitochondrial antioxidant network with the TRX2 inhibitor gentian violet or the thiazole antibiotic thiostrepton leads to intolerable levels of mitochondrial oxidants, loss of FOXM1 expression, and MM cell death (Newick et al., 2012).

Rehman et al. (2012) have recently shown that expression of the mitochondrial fission regulator DRP1 is elevated in lung cancer, with a loss of mitochondrial tubular networks being a phenotypic signature of this tumor. Promoting mitochondrial fusion reduced the growth of lung cancer cells in vitro, and impeded tumor growth in vivo (Rehman et al., 2012), indicating that increased mitochondrial fission has pro-tumorigenic effects. The phenotypic properties of MM and LP9 cells are similar in that we also have observed that the mitochondria in MM cells tend to be less tubular and are predominantly small and vesicular, whereas LP9 and primary human mesothelial cells contain mitochondria with a more trabecular organization (data not shown). Similar studies on expression and activity of DRP1 in MM cells will be required to determine if enhanced mitochondrial fission is a characteristic of MM.

Although MT and MCP have been shown to block increases in oxidant levels both in vitro and cellular systems, their effects appear to be dose-dependent and vary depending on cell type. At similar concentrations as used herein (1–5 μM) MCP has been shown to inhibit H_2O_2-induced oxidative damage in

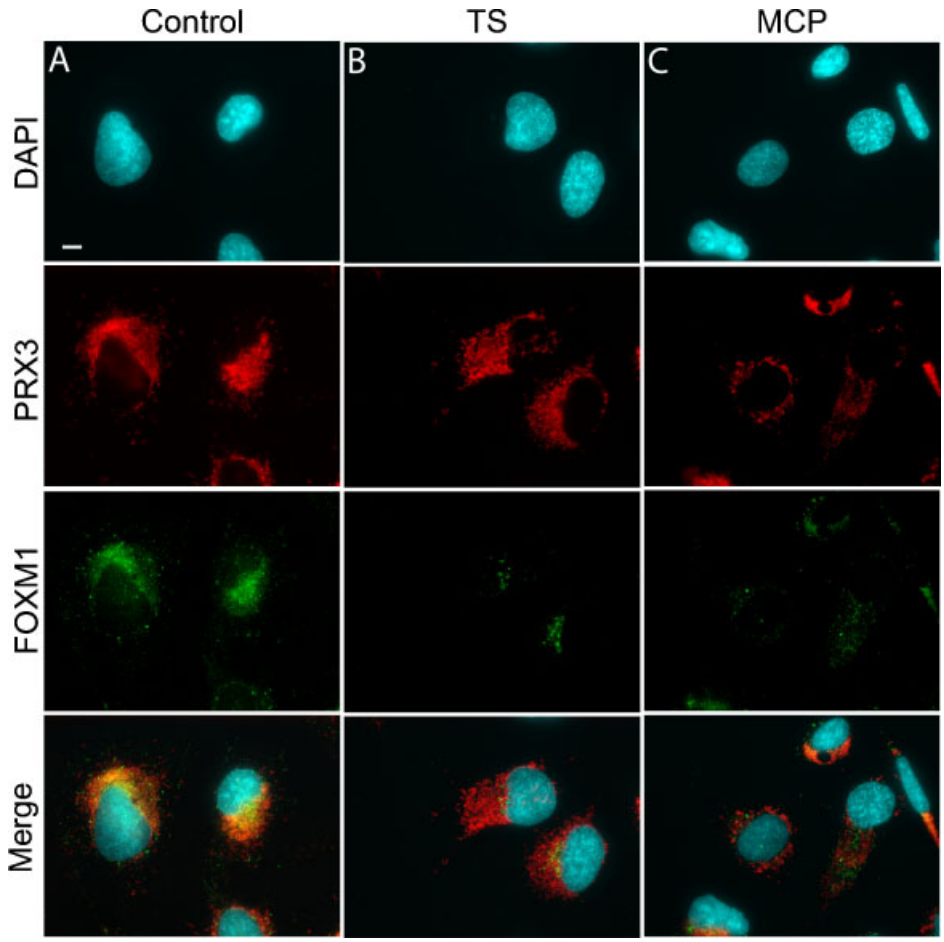

Fig. 7. FOXM1 and PRX3 coexist in the cytoplasm of HM cells. Scale bar = 10 μm. A: HM cells were processed for immunofluorescence microscopy using the indicated primary antibodies; nuclear DNA was stained with DAPI. B: HM cells were treated for 18 h with 1 μM TS and stained for subcellular localization of FOXM1 and PRX3 as in column A. C: HM cells were treated for 18 h with 1 μM MCP and stained for subcellular localization of FOXM1 as in column A. As detected in by immunoblotting, TS reduced the signal for FOXM1 without affecting PRX3, whereas MCP reduced the signal for FOXM1 and PRX3.

endothelial cells (Dhanasekaran et al., 2005). Weinberg et al. (2010) have attributed the ability of MCP to inhibit tumor growth in a KRAS driven mouse tumor model to inhibition of oxidant-dependent signaling, but their data also indicate that MCP leads to hyper-phosphorylation of ERK1/2, a MAPK exquisitely responsive to increased oxidative stress (Burch et al., 2004). Others have shown that Mito-Q, a mitochondrial targeted form of the antioxidant ubiquinone, is very effective at reducing mitochondria-derived oxidants and reducing lipid peroxidation (Kelso et al., 2001; Asin-Cayuela et al., 2004; Smith et al., 2011). In contrast Mukherjee et al. (2007) and O'Malley et al. (2006) have shown that Mito-Q is capable of increasing oxidant production in cellular systems and isolated mitochondria, and that the carbohydrate source for fueling the organelle had varying effects on the production of oxidants.

Here, live cell imaging with mito-roGFP2 showed that both MCP and MT dramatically alter mitochondrial architecture at concentrations that result in increased production of mitochondrial oxidants, suggesting that MCP and MT may perturb enzymes present in the ETC in MM cell mitochondria, as has been reported for other compounds targeted to mitochondria by the TPP moiety (O'Malley et al., 2006). The evidence that TPP compounds can perturb mitochondrial membrane dynamics was shown in the early 1990's (Rideout et al., 1994; Manetta et al., 1996) but susceptible protein targets were not described. MCP and MT, but not CP, TEMPOL, or TPP, increased mitochondrial-derived oxidants (Fig. 2B), inhibited ATP production (Fig. 3F) and decreased mitochondrial membrane potential in MM cells (Fig. 3G). Disruption of mitochondrial architecture with MCP also increased levels of hyper-oxidized 2-Cys peroxiredoxins (Fig. 2C), and over short time periods increased the levels of disulfide-bonded dimers of PRX3 (Fig. 2D), signatures of increased oxidative stress. These phenotypic effects do not appear to result from induction of mitochondrial fission, for the lasso and ring-like mitochondrial structures observed in response to these compounds are not characteristic of mitochondrial fission (Oettinghaus et al., 2011), and pre-treatment of cells with mdivi-1 did not attenuate the effects of MCP on mitochondrial fragmentation and the reduction in form factor (Fig. 3D). Electron microscopy suggests that swelling of the mitochondrial matrix leads to protein degradation and disruption of electron chain dynamics.

Several of the compounds we have investigated to date that target mitochondria affect expression of FOXM1, but only MCP and MT decreased expression of PRX3. Over the short-time intervals studied here, MCP did not affect PRX3 mRNA levels

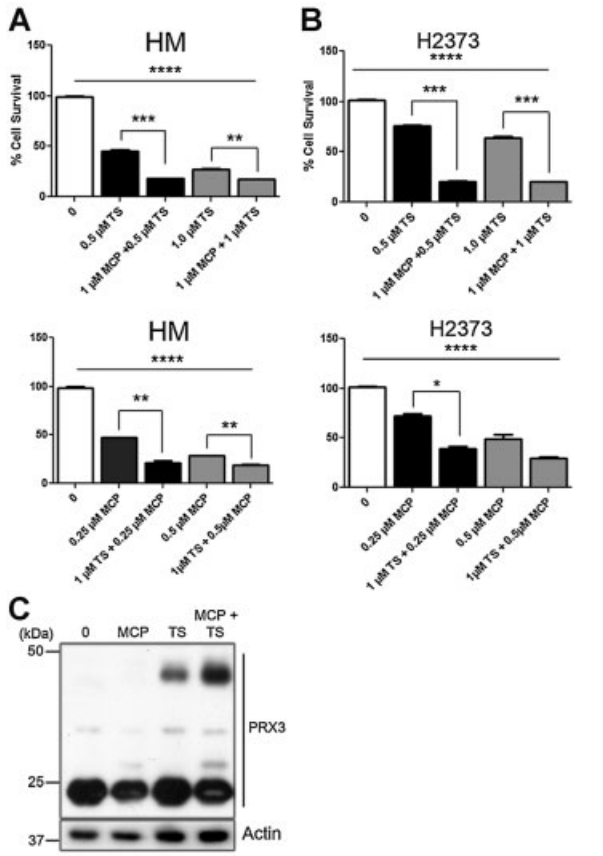

Fig. 8. MCP inhibits cell viability and potentiates the cytotoxic effects of TS. HM (A) and H2373 (B) cells were treated with the indicated concentrations of MCP, TS, or MCP and TS for 3 days and total cell mass was quantified by solubilizing crystal violet stain. The data are presented as % cell survival as compared to untreated controls (0 drug dose). Overall changes in each group were statistically analyzed by one-way ANOVA (n = 3, $^{****}P = 0.0001$), while differences between treatment groups were statistically analyzed by Student's *t*-test (n = 3, $^{***}P = 0.001$, $^{**}P = 0.003$, $^{*}P = 0.01$). C: HM cells were treated with 1 μM MCP, 1 μM TS, or 1 μM MCP + 1 μM TS as indicated for 18 h, and cell lysates were examined for PRX3 expression by immunoblotting. MCP potentiates the ability of TS to modify PRX3, leading to a SDS and DTT-resistant species that migrates at ~50 kDa (Newick et al., 2012).

(data not shown), but clearly decreased PRX3 expression as detected by immunoblotting and IF. MCP promotes oxidation of PRX protein (Fig. 2C), which may enhance PRX3 proteolytic destruction by Lon protease (Bota and Davies, 2002). We have not investigated the levels or activity of sulfiredoxin, which repairs hyper-oxidized PRX3, so presently it is unclear if PRX3-SO_2H is repaired over time in MM cells. While several compounds over time increase the relative levels of mitochondrial oxidants (i.e., gentian violet, TS, MCP, and MT), the results with PRX3 indicate it is unlikely that a common mechanism is responsible for inhibition of FOXM1 by each agent. Immunofluorescence experiments indicate that a significant fraction of cellular FOXM1 is associated with mitochondria in the MM cell cytoplasm, which may link mitochondrial oxidant production and metabolism to FOXM1. However, a much better understanding of the expression, modification, subcellular trafficking, and turnover of specific FOXM1 isoforms will be required to deduce the mechanism of each agent. Nonetheless, certain combinations of agents that influence mitochondrial function are more cytotoxic than either compound alone. For example, like gentian violet, MCP promotes the adduction of PRX3 by TS (Fig. 8C), and each has either a synergistic or additive effect with TS on MM cell cytotoxicity. These findings indicate that combinations of compounds that act through complementary mechanisms on mitochondrial physiology may prove effective at lower doses, with fewer collateral effects on normal cells.

Acknowledgments

We thank the University of Vermont Microscopy Imaging Center and the Advanced Genome Technology Core of the Vermont Cancer Center for technical assistance. The humanized redox-responsive GFP targeted to mitochondria (Mito-roGFP) was a generous gift provided by J. Andre Melendez, whose laboratory generated this construct based on work originally reported by S. Jim Remington (Cannon and Remington, 2006). This work was supported by the John Sterling Memorial Grant from the Mesothelioma Applied Research Foundation, the Lake Champlain Cancer Research Organization, the Vermont Ladies Auxiliary of Veterans of Foreign Wars, and the Vermont Cancer Center. K.N. was supported by a training grant in Environmental Pathology from the NIEHS (T32 ES007122-29).

Literature Cited

Antico Arciuch VG, Elguero ME, Poderoso JJ, Carreras MC. 2012. Mitochondrial regulation of cell cycle and proliferation. Antioxid Redox Signal 16:1150–1180.
Asin-Cayuela J, Manas AR, James AM, Smith RA, Murphy MP. 2004. Fine-tuning the hydrophobicity of a mitochondria-targeted antioxidant. FEBS Lett 571:9–16.
Berger KH, Yaffe MP. 1996. Mitochondrial distribution and inheritance. Experientia 52:1111–1116.
Bhat UG, Halasi M, Gartel AL. 2009. Thiazole antibiotics target FoxM1 and induce apoptosis in human cancer cells. PLoS ONE 4:e5592.
Bota DA, Davies KJ. 2002. Lon protease preferentially degrades oxidized mitochondrial aconitase by an ATP-stimulated mechanism. Nat Cell Biol 4:674–680.
Burch PM, Yuan Z, Loonen A, Heintz NH. 2004. An extracellular signal-regulated kinase 1- and 2-dependent program of chromatin trafficking of c-Fos and Fra-1 is required for cyclin D1 expression during cell cycle reentry. Mol Cell Biol 24:4696–4709.
Burhans WC, Heintz NH. 2009. The cell cycle is a redox cycle: Linking phase-specific targets to cell fate. Free Radic Biol Med 47:1282–1293.
Cannon MB, Remington SJ. 2006. Re-engineering redox-sensitive green fluorescent protein for improved response rate. Protein Sci 15:45–57.
Cassidy-Stone A, Chipuk JE, Ingerman E, Song C, Yoo C, Kuwana T, Kurth MJ, Shaw JT, Hinshaw JE, Green DR, Nunnari J. 2008. Chemical inhibition of the mitochondrial division dynamin reveals its role in Bax/Bak-dependent mitochondrial outer membrane permeabilization. Dev Cell 14:193–204.
Cheng G, Zielonka J, Dranka BP, McAllister D, Mackinnon AC, Jr., Joseph J, Kalyanaraman B. 2012. Mitochondria-targeted drugs synergize with 2-deoxyglucose to trigger breast cancer cell death. Cancer Res 72:2634–2644.
Conour JE, Graham WV, Gaskins HR. 2004. A combined in vitro/bioinformatic investigation of redox regulatory mechanisms governing cell cycle progression. Physiol Genomics 18:196–205.
Cox AG, Pearson AG, Pullar JM, Jonsson TJ, Lowther WT, Winterbourn CC, Hampton MB. 2009a. Mitochondrial peroxiredoxin 3 is more resilient to hyperoxidation than cytoplasmic peroxiredoxins. Biochem J 421:51–58.
Cox AG, Peskin AV, Paton LN, Winterbourn CC, Hampton MB. 2009b. Redox potential and peroxide reactivity of human peroxiredoxin 3. Biochemistry 48:6495–6501.
Cox AG, Winterbourn CC, Hampton MB. 2009c. Mitochondrial peroxiredoxin involvement in antioxidant defence and redox signalling. Biochem J 425:313–325.
de Oliveira MF, Amoedo ND, Rumjanek FD. 2012. Energy and redox homeostasis in tumor cells. Int J Cell Biol 2012:593838.
Dhanasekaran A, Kotamraju S, Karunakaran C, Kalivendi SV, Thomas S, Joseph J, Kalyanaraman B. 2005. Mitochondria superoxide dismutase mimetic inhibits peroxide-induced oxidative damage and apoptosis: Role of mitochondrial superoxide. Free Radic Biol Med 39:567–583.
Diaz-Ruiz R, Rigoulet M, Devin A. 2011. The Warburg and Crabtree effects: On the origin of cancer cell energy metabolism and of yeast glucose repression. Biochim Biophys Acta 1807:568–576.
Droge W. 2002. Free radicals in the physiological control of cell function. Physiol Rev 82:47–95.
Fischer F, Hamann A, Osiewacz HD. 2012. Mitochondrial quality control: An integrated network of pathways. Trends Biochem Sci 37:284–292.
Fried L, Arbiser JL. 2008. The reactive oxygen-driven tumor: Relevance to melanoma. Pigment Cell Melanoma Res 21:117–122.
Friedrich T, Van Heek P, Leif H, Ohnishi T, Forche E, Kunze B, Jansen R, Trowitzsch-Kienast W, Höfle G, Reichenbach H, Weiss H. 1994. Two binding sites of inhibitors in NADH: Ubiquinone oxidoreductase (complex I). Relationship of one site with the ubiquinone-binding site of bacterial glucose:ubiquinone oxidoreductase. Eur J Biochem 219:691–698.
Gupta SC, Hevia D, Patchva S, Park B, Koh W, Aggarwal BB. 2012. Upsides and downsides of reactive oxygen species for cancer: The roles of reactive oxygen species in tumorigenesis, prevention, and therapy. Antioxid Redox Signal 16:1295–1322.
Hamanaka RB, Chandel NS. 2010. Mitochondrial reactive oxygen species regulate cellular signaling and dictate biological outcomes. Trends Biochem Sci 35:505–513.

Hanson GT, Aggeler R, Oglesbee D, Cannon M, Capaldi RA, Tsien RY, Remington SJ. 2004. Investigating mitochondrial redox potential with redox-sensitive green fluorescent protein indicators. J Biol Chem 279:13044–13053.
Janssen-Heininger YM, Mossman BT, Heintz NH, Forman HJ, Kalyanaraman B, Finkel T, Stamler JS, Rhee SG, van der Vliet A. 2008. Redox-based regulation of signal transduction: Principles, pitfalls, and promises. Free Radic Biol Med 45:1–17.
Jones DP. 2006. Disruption of mitochondrial redox circuitry in oxidative stress. Chem Biol Interact 163:38–53.
Jones DP. 2010. Redox sensing: Orthogonal control in cell cycle and apoptosis signalling. J Intern Med 268:432–448.
Kalyanaraman B, Darley-Usmar V, Davies KJ, Dennery PA, Forman HJ, Grisham MB, Mann GE, Moore K, Roberts LJ II, Ischiropoulos H. 2011. Measuring reactive oxygen and nitrogen species with fluorescent probes: Challenges and limitations. Free Radic Biol Med 52:1–6.
Kelso GF, Porteous CM, Coulter CV, Hughes G, Porteous WK, Ledgerwood EC, Smith RAJ, Murphy MP. 2001. Selective targeting of a redox-active ubiquinone to mitochondria within cells. J Biol Chem 276:4588–4596.
Khan SA, Nanduri J, Yuan G, Kinsman B, Kumar GK, Joseph J, Kalyanaraman B, Prabhakar NR. 2011. NADPH oxidase 2 mediates intermittent hypoxia-induced mitochondrial complex I inhibition: Relevance to blood pressure changes in rats. Antioxid Redox Signal 14:533–542.
Klaunig JE, Wang Z, Pu X, Zhou S. 2011. Oxidative stress and oxidative damage in chemical carcinogenesis. Toxicol Appl Pharmacol 254:86–99.
Koopman WJ, Verkaart S, Visch HJ, van der Westhuizen FH, Murphy MP, van den Heuvel LW, Smeitink JA, Willems PH. 2005. Inhibition of complex I of the electron transport chain causes O_2-mediated mitochondrial outgrowth. Am J Physiol Cell Physiol 288:C1440–C1450.
Koopman WJ, Visch HJ, Smeitink JA, Willems PH. 2006. Simultaneous quantitative measurement and automated analysis of mitochondrial morphology, mass, potential, and motility in living human skin fibroblasts. Cytometry A 69:1–12.
Laoukili J, Stahl M, Medema RH. 2007. Fox M1: At the crossroads of ageing and cancer. Biochim Biophys Acta 1775:92–102.
Laoukili J, Alvarez-Fernandez M, Stahl M, Medema RH. 2008. FoxM1 is degraded at mitotic exit in a Cdh1-dependent manner. Cell Cycle 7:2720–2726.
Lee AC, Fenster BE, Ito H, Takeda K, Bae NS, Hirai T, Yu ZX, Ferrans VJ, Howard BH, Finkel T. 1999. Ras proteins induce senescence by altering the intracellular levels of reactive oxygen species. J Biol Chem 274:7936–7940.
Ma RY, Tong TH, Cheung AM, Tsang AC, Leung WY, Yao KM. 2005. Raf/MEK/MAPK signaling stimulates the nuclear translocation and transactivating activity of FOXM1c. J Cell Sci 118:795–806.
Manetta A, Gamboa G, Nasseri A, Podnos YD, Emma D, Dorion G, Rawlings L, Carpenter PM, Bustamante A, Patel J, Rideout D. 1996. Novel phosphonium salts display in vitro and in vivo cytotoxic activity against human ovarian cancer cell lines. Gynecol Oncol 60:203–212.
Millard M, Pathania D, Shabaik Y, Taheri L, Deng J, Neamati N. 2010. Preclinical evaluation of novel triphenylphosphonium salts with broad-spectrum activity. PLoS ONE 5:e13131.
Miller EW, Tulyathan O, Isacoff EY, Chang CJ. 2007. Molecular imaging of hydrogen peroxide produced for cell signaling. Nat Chem Biol 3:263–267.
Mitra K, Wunder C, Roysam B, Lin G, Lippincott-Schwartz J. 2009. A hyperfused mitochondrial state achieved at G1-S regulates cyclin E buildup and entry into S phase. Proc Natl Acad Sci USA 106:11960–11965.
Modica-Napolitano JS, Aprille JR. 2001. Delocalized lipophilic cations selectively target the mitochondria of carcinoma cells. Adv Drug Deliv Rev 49:63–70.
Mukherjee TK, Mishra AK, Mukhopadhyay S, Hoidal JR. 2007. High concentration of antioxidants N-acetylcysteine and mitoquinone-Q induces intercellular adhesion molecule 1 and oxidative stress by increasing intracellular glutathione. J Immunol 178:1835–1844.
Murphy MP. 1997. Selective targeting of bioactive compounds to mitochondria. Trends Biotechnol 15:326–330.
Murphy MP. 2009. How mitochondria produce reactive oxygen species. Biochem J 417:1–13.
Myatt SS, Lam EW. 2007. The emerging roles of forkhead box (Fox) proteins in cancer. Nat Rev 7:847–859.
Newick K, Cunniff B, Preston K, Held P, Arbiser J, Pass H, Mossman B, Shukla A, Heintz N. 2012. Peroxiredoxin 3 is a redox-dependent target of thiostrepton in malignant mesothelioma cells. PLoS ONE 7:e39404.
Oettinghaus B, Licci M, Scorrano L, Frank S. 2011. Less than perfect divorces: Dysregulated mitochondrial fission and neurodegeneration. Acta Neuropathol 123:189–203.
O'Malley Y, Fink BD, Ross NC, Prisinzano TE, Sivitz WI. 2006. Reactive oxygen and targeted antioxidant administration in endothelial cell mitochondria. J Biol Chem 281:39766–39775.
Pandit B, Gartel AL. 2011. FoxM1 knockdown sensitizes human cancer cells to proteasome inhibitor-induced apoptosis but not to autophagy. Cell Cycle (Georgetown, Texas) 10:3269–3273.
Park HJ, Costa RH, Lau LF, Tyner AL, Raychaudhuri P. 2008. Anaphase-promoting complex/cyclosome-CDH1-mediated proteolysis of the forkhead box M1 transcription factor is critical for regulated entry into S phase. Mol Cell Biol 28:5162–5171.
Park HJ, Carr JR, Wang Z, Nogueira V, Hay N, Tyner AL, Lau LF, Costa RH, Raychaudhuri P. 2009. FoxM1, a critical regulator of oxidative stress during oncogenesis. EMBO J 28:2908–2918.
Pass HI, Stevens EJ, Oie H, Tsokos MG, Abati AD, Fetsch PA, Mew DJ, Pogrebniak HW, Matthews WJ. 1995. Characteristics of nine newly derived mesothelioma cell lines. Ann Thorac Surg 59:835–844.
Phalen TJ, Weirather K, Deming PB, Anathy V, Howe AK, van der Vliet A, Jonsson TJ, Poole LB, Heintz NH. 2006. Oxidation state governs structural transitions in peroxiredoxin II that correlate with cell cycle arrest and recovery. J Cell Biol 175:779–789.
Qiao S, Lamore SD, Cabello CM, Lesson JL, Munoz-Rodriguez JL, Wondrak GT. 2012. Thiostrepton is an inducer of oxidative and proteotoxic stress that impairs viability of human melanoma cells but not primary melanocytes. Biochem Pharmacol 83:1229–1240.
Ralph SJ, Rodriguez-Enriquez S, Neuzil J, Saavedra E, Moreno-Sanchez R. 2010. The causes of cancer revisited: "mitochondrial malignancy" and ROS-induced oncogenic transformation—Why mitochondria are targets for cancer therapy. Mol Aspects Med 31:145–170.
Reale FR, Griffin TW, Compton JM, Graham S, Townes PL, Bogden A. 1987. Characterization of a human malignant mesothelioma cell line (H-MESO-1): A biphasic solid and ascitic tumor model. Cancer Res 47:3199–3205.
Rehman J, Zhang HJ, Toth PT, Zhang Y, Marsboom G, Hong Z, Salgia R, Husain AN, Wietholt C, Archer SL. 2012. Inhibition of mitochondrial fission prevents cell cycle progression in lung cancer. FASEB J 26:2175–2186.
Rhee SG. 2006. Cell signaling. H_2O_2, a necessary evil for cell signaling. Science 312:1882–1883.
Rideout D, Bustamante A, Patel J. 1994. Mechanism of inhibition of FaDu hypopharyngeal carcinoma cell growth by tetraphenylphosphonium chloride. Int J Cancer 57:247–253.
Shenouda SM, Widlansky ME, Chen K, Xu G, Holbrook M, Tabit CE, Hamburg NM, Frame AA, Caiano TL, Kluge MA, Duess M-A, Levit A, Kim B, Hartman M-L, Joseph L, Shirihai OS, Vita JA. 2011. Altered mitochondrial dynamics contributes to endothelial dysfunction in diabetes mellitus/clinical perspective. Circulation 124:444–453.
Shukla A, Jung M, Stern M, Fukagawa NK, Taatjes DJ, Sawyer D, Van Houten B, Mossman BT. 2003. Asbestos induces mitochondrial DNA damage and dysfunction linked to the development of apoptosis. Am J Physiol Lung Cell Mol Physiol 285:L1018–L1025.
Smith RAJ, Hartley RC, Murphy MP. 2011. Mitochondria-targeted small molecule therapeutics and probes. Antioxid Redox Signal 15:3021–3038.
Taguchi N, Ishihara N, Jofuku A, Oka T, Mihara K. 2007. Mitotic phosphorylation of dynamin-related GTPase Drp1 participates in mitochondrial fission. J Biol Chem 282:11521–11529.
Tait SW, Green DR. 2010. Mitochondria and cell signalling. J Cell Sci 125:807–815.
Trnka J, Blaikie FH, Smith RA, Murphy MP. 2008. A mitochondria-targeted nitroxide is reduced to its hydroxylamine by ubiquinol in mitochondria. Free Radic Biol Med 44:1406–1419.
Venkatesh S, Lee J, Singh K, Lee I, Suzuki CK. 2011. Multitasking in the mitochondrion by the ATP-dependent Lon protease. Biochim Biophys Acta 1823:56–66.
Wang Z, Ahmad A, Li Y, Banerjee S, Kong D, Sarkar FH. 2010. Forkhead box M1 transcription factor: A novel target for cancer therapy. Cancer Treat Rev 36:151–156.
Weinberg F, Hamanaka R, Wheaton WW, Weinberg S, Joseph J, Lopez M, Kalyanaraman B, Mutlu GM, Budinger GR, Chandel NS. 2010. Mitochondrial metabolism and ROS generation are essential for Kras-mediated tumorigenicity. Proc Natl Acad Sci USA 107:8788–8793.
Yu T, Jhun BS, Yoon Y. 2011. High-glucose stimulation increases reactive oxygen species production through the calcium and mitogen-activated protein kinase-mediated activation of mitochondrial fission. Antioxid Redox Signal 14:425–437.
Zhang X, Zheng Y, Fried LE, Du Y, Montano SJ, Sohn A, Lefkove B, Holmgren L, Arbiser JL, Holmgren A, Lu J. 2011. Disruption of the mitochondrial thioredoxin system as a cell death mechanism of cationic triphenylmethanes. Free Radic Biol Med 50:811–820.